Laser-treated substrate with nanoparticles for surface-enhanced Raman scattering

Cheng-Hsiang Lin,[1,2] Lan Jiang,[3] Jun Zhou,[4] Hai Xiao,[5] Shean-Jen Chen,[1] and Hai-Lung Tsai[2,*]

[1]*Department of Engineering Science, National Cheng Kung University, Tainan 70101, Taiwan*
[2]*Department of Mechanical and Aerospace Engineering, Missouri University of Science and Technology, Rolla, Missouri 65409, USA*
[3]*Department of Mechanical and Automation Engineering, 3rd School, Beijing Institute of Technology, Beijing, 100081, China*
[4]*Department of Mechanical Engineering, The Pennsylvania State University Erie, 1501 Jordan Road, Erie, Pennsylvania 16563, USA*
[5]*Department of Electrical and Computer Engineering, Missouri University of Science and Technology, Rolla, Missouri 65409, USA*
**Corresponding author: tsai@mst.edu*

Received December 8, 2009; revised January 25, 2010; accepted February 3, 2010; posted February 26, 2010 (Doc. ID 121142); published March 19, 2010

A rapid and simple approach to fabricate a large area of nanostructured substrate for surface-enhanced Raman scattering (SERS) is reported. Gold nanoparticles ranging from 10 to 40 nm in diameter uniformly distributed on a silicon substrate were obtained by annealing the gold film precoated on the silicon substrate with UV nanosenond (ns) laser pulses. The gold nanoparticles were formed by surface tension of the melted gold layer heated by ns laser pulses. The enhancement factor of the SERS substrate for Rhodamine 6G at 632.8 nm excitation was measured to be higher than 10^5. The proposed technique provides the opportunity to equip a functional microchip with SERS capability of high sensitivity and chemical stability. © 2010 Optical Society of America

OCIS codes: 300.6450, 240.6695.

Since surface-enhanced Raman scattering (SERS) was discovered three decades ago [1,2], the technique has been widely employed for molecular detection owing to its capabilities of simultaneously providing the structural [3] and quantitative [4,5] information, as well as high sensitivity for single molecular detection [6]. Because the enhancement factors (EFs) depend on the properties of metal nanostructures, such as surface morphology, types of metals, and chemical environment of the nanostructures, a variety of approaches have been developed to fabricate SERS substrates, including electrochemically roughened electrodes, aggregates of colloidal gold or silver particles, and nanolithography, with the expectation of obtaining higher EFs [7].

In general, noble metals are commonly used for SERS applications due to their favorable optical properties [8]. Silver has the leading EF among many kinds of metals but its chemical instability is an intrinsic drawback. Although the EF of gold is not as high as silver, its high chemical stability and molecular compatibility are the major advantages. In this Letter, we develop a rapid and effective approach to produce controllable gold nanoparticle arrays on substrates over a large area for SERS applications, which provides a high EF and high chemical stability. Using the annealing process conducted in open air and at room temperature by the UV nanosecond (ns) laser pulses, gold films precoated on silicon substrates are rapidly transformed into gold nanoparticle arrays with fairly uniform distributions of particle size and interparticle spacing. By using Rhodamine 6G (R6G) as the analyte molecules at the excitation wavelength of 632.8 nm, the substrate fabricated by this approach provides a high EF of 10^5.

The experiment was carried out with a ns laser micromachining system that consists of a frequency-tripled Nd:YAG ns laser (AVIA 355-X, Coherent), a computer-controlled four-axis motion stage (Aerotech). The central wavelength, maximum repetition rate, and pulse width of the ns laser are 355 nm, 300 kHz, and 30 ns, respectively. The pulse energy to meet different experimental requirements was adjusted by a combination of a half-wave plate and a linear polarizer.

A 10 nm gold film was coated on the cleaned flat silicon substrate via an rf sputtering coater. The coated substrate was translated by the motion stage during the laser annealing process at room temperature and in open air. The repetition rate and pulse energy used in this work were, respectively, 10 kHz and 130 μJ. The UV laser pulses were focused onto the sample by a planoconvex lens with 75 mm focal length to achieve the energy density of 265 mJ/cm^2 in an area of 250 μm in diameter. The scanning speed was set as 10 mm/min, which corresponds to 15,000 pulse/area in the spot area. For comparison purpose, a substrate with the same condition of 10 nm gold film was also treated by thermal annealing in a furnace ramping from room temperature to 1000°C at 10°C/min and holding at 1000°C for 10 min. After the laser or thermal annealing process, the sample was examined by a scanning electron microscope (SEM).

In SERS measurements, aqueous solutions of R6G with concentrations of 10^{-3} M and 10^{-6} M were utilized as analyte molecules to calibrate the EFs. The

prepared solution was cast on the SERS substrate using a pipette. The solutions were covered by a microscope cover slip to ensure a uniform thickness of the R6G solution layer and to minimize solvent evaporation. The SERS measurements were conducted by a commercial Ramanscope (Jobin Yvon) using a He–Ne laser as an exciting light source. The employed exciting power and the signal accumulation time were adjustable. The objective lens and grating used in this work were, respectively, 10× (NA=0.25) and 600 line/mm.

Figure 1(a) shows the SEM image of the gold nanoparticles produced by thermal annealing. The average particle size is 562.0 nm with standard deviation of 136.7 nm, Fig. 1(b), and the interparticle spacing is in the range of a few micrometers. After the gold film was treated by low fluence (150 mJ/cm^2) ns laser pulses, the gold film was fragmented into large pieces at random locations and each piece is balled into a single large droplet, Fig. 1(c). To assure there are no small nanoparticles at the no-particle area of Fig. 1(c), the area was enlarged and confirmed. The average diameter and standard deviation of particles in Fig. 1(c) are respectively 329.8 nm and 78.7 nm, Fig. 1(d). As the fluence of the ns laser pulse is increased to 265 mJ/cm^2, bigger particles no longer exist; instead, dense and uniform particles appear as shown in Fig. 1(e). Figure 1(f) shows the averaged particle diameter and standard deviation, which are 30.8 nm and 8.0 nm, respectively. The distribution of the nanoparticle diameter in Fig. 1(f) consists of two major groups whose peaks are, respectively, at 20 nm and 35 nm, and the 35 nm peak appears to be the major particle size.

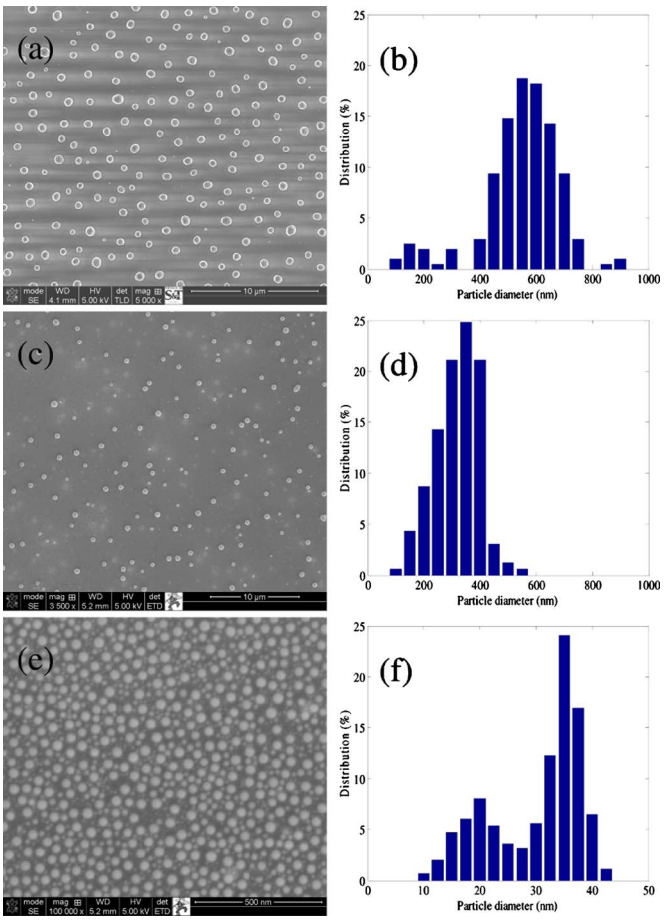

Fig. 1. (Color online) SEM images of the gold nanoparticle arrays (a) fabricated by thermal annealing; (b) size distribution of (a); (c) fabricated by ns laser annealing at 150 mJ/cm^2; (d) size distribution of (c); (e) fabricated by ns laser annealing at 265 mJ/cm^2; (f) size distribution of (e).

For thermal annealing, the gold film and substrate were heated slowly in a furnace, and the gold film started breaking into pieces when the temperature reached around 700°C. The broken gold films were continuously heated, allowing enough time for the surface tension to act and the melted gold layer to form large particles. In contrast, when treated by ns laser pulses the gold film experiences rapid heating and cooling due to short laser–film interactions. Although metal nanoparticles generated by irradiating the metal film with ns laser pulses have been theoretically studied based on the heat conduction analysis [9] and hydrodynamic model [10] and possible mechanisms, such as dewetting and thermocapillary instability [10,11] were proposed, detailed mechanisms leading to the formation of uniform nanoparticles are still unclear and need additional investigations. If the laser fluence exceeds the damage threshold, which is about 290 mJ/cm^2, the silicon substrate along with the gold film will be ablated and there are almost no gold nanoparticles found on the surface of the ablated substrate.

Figure 2 shows the SERS spectra of 10^{-6} M R6G measured on the silicon substrate coated with 10 nm gold film before annealing [trace (a)], after thermal annealing [trace (b)], after laser treating at 150 mJ/cm^2 [trace (c)], and after laser treating at 265 mJ/cm^2 [trace (d)]. Trace (e) of Fig. 2 is the normal Raman spectrum of 10^{-3} M R6G measured on

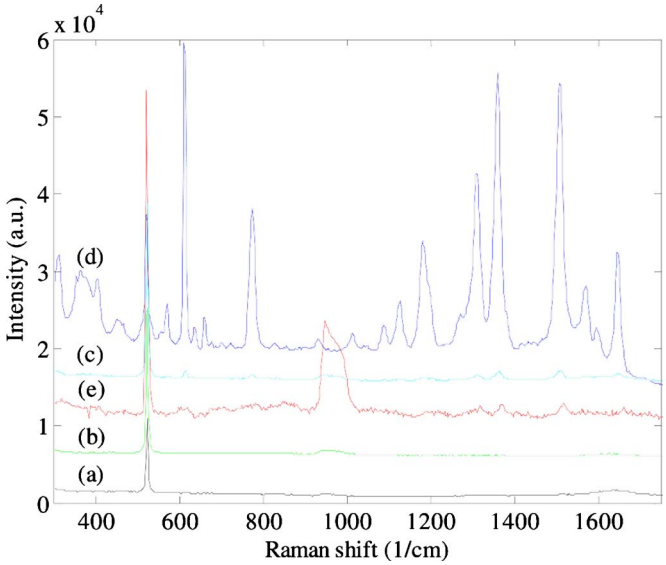

Fig. 2. (Color online) SERS spectra of the 10^{-6} M R6G measured on a 10 nm gold film (a) before thermal annealing, (b) after thermal annealing, (c) after laser annealing at 150 mJ/cm^2, and (d) after laser annealing at 265 mJ/cm^2. (e) Normal Raman spectra of 10^{-3} M R6G measured on the surface of the bare silicon substrate.

the bare silicon substrate. For SERS [traces (a) through (d)] and normal Raman [trace (e)] spectra, the exciting powers are, respectively, 8.5 mW and 17 mW, and the accumulating times are, respectively, 5 s and 30 s. It is seen that the SERS spectra at the fluence of 265 mJ/cm^2 are significantly greater than those at 150 mJ/cm^2. There is no apparent signal of R6G before annealing and after thermal annealing. Hence, the strong signal enhancement must be caused by the laser annealed gold nanoparticles. In Fig. 1, the nanoparticles produced by ns laser pulses at 265 mJ/cm^2 with a major diameter of 35 nm are suitable for localized surface plasmon at the visible light range [12], which contributes to the EM field enhancement resulting in high EFs. Furthermore, the interparticle spacing is in the range of tens of nanometers, which is consistent with the previous studies that the signal enhancement increases with the decrease of interparticle spacing [13]. In the normal Raman spectrum of 10^{-3} M R6G, weak R6G signals are seen. Note that the strong sharp peak at 520 cm^{-1} and the broad peak from 950 cm^{-1} to 1000 cm^{-1} are inherited from the silicon substrate [14]. The signals of bare silicon substrate [trace (e)] are strong owing to the higher exciting power and longer accumulating time. However, the signals of bare silicon are also visible in the SERS spectrum, although the intensities are much lower.

To quantify the performance of the SERS substrate, the SERS signal of 10^{-6} M R6G measured on the annealed sample by laser pulses [trace (d)] is compared with the normal Raman signal of 10^{-3} M R6G measured on the bare silicon surface [trace (e)]. The commonly accepted EF is defined by the following equation:

$$EF = \frac{I_{SERS}}{N_{SERS}} \Big/ \frac{I_{nR}}{N_{nR}}, \tag{1}$$

where I_{nR} and I_{SERS} are, respectively, the intensities of normal Raman and SERS in the unit of $mW^{-1}\ s^{-1}$ [15]. Note that in Eq. (1) the intensity of exciting laser and the accumulating time have been normalized with respect to the exciting laser power and accumulating time for both the SERS and normal Raman spectra. N_{nR} and N_{SERS} represent, respectively, the number of molecules probed on the reference sample and on the SERS substrate. Assuming the effective surface areas of the substrates with and without nanoparticles are identical, and there is no specific binding between the analyte and the sample surface, the number of adsorbent molecules on the surface is proportional to the concentration of the analyte solution in which the samples were incubated. Calculated by Eq. (1) with the aforementioned assumption and conditions, the EFs at Raman peaks 610 cm^{-1}, 1310 cm^{-1}, 1363 cm^{-1}, and 1509 cm^{-1} are estimated to be 3.9×10^5, 2.9×10^5, 3.9×10^5 and 3.2×10^5, respectively, demonstrating the high sensitivity. Note the data were all measured on the center area of the annealed region. Compared with the silver-based SERS substrates, the chemical stability of gold allows a wider range of analyte molecules and is easier for storing the fabricated substrates.

In summary, this Letter reports a rapid and efficient method to fabricate the SERS substrates in a large area with high chemical stability and high EFs. The gold nanoparticles were annealed from the coated gold film on silicon substrates by ns laser pulses. The particle distribution and particle size are dense and uniform on the substrate, leading to a high EF of 10^5. The chemical stability of gold would broaden the SERS applications in biomedical and analytical chemistry.

This work was partially supported by the U.S. Department of Energy under contract DE-FE0001127 and the National Natural Science Foundation of China (NSFC) under grant 90923039.

References

1. M. Fleischmann, P. J. Hendra, and A. J. McQuillan, Chem. Phys. Lett. **26**, 163 (1974).
2. D. L. Jeanmaire and R. P. Van Duyne, J. Electroanal. Chem. **84**, 1 (1977).
3. C. Fang, A. Agarwal, K. D. Buddharaju, N. M. Khalid, S. M. Salim, E. Widjaja, M. V. Garland, N. Balasubramanian, and D. L. Kwong, Biosens. Bioelectron. **24**, 216 (2008).
4. D. Meason, L. Seballos, D. Yin, J. Z. Zhang, E. J. Lunt, A. R. Hawkins, and H. Schmidt, Appl. Phys. Lett. **90**, 211107 (2007).
5. L. Su, C. J. Rowlands, and S. R. Elliott, Opt. Lett. **34**, 1645 (2007).
6. K. Kneipp, Y. Wang, H. Kneipp, L. T. Perelman, I. Itzkan, R. R. Dasari, and M. S. Feld, Phys. Rev. Lett. **78**, 1667 (1997).
7. R. J. C. Brown and J. T. Milton, J. Raman Spectrosc. **39**, 1313 (2008).
8. M. Kerker, J. Opt. Soc. Am. B **2**, 1327 (1985).
9. S. J. Henley, J. D. Carey, and S. R. P. Silva, Phys. Rev. B **72**, 195408 (2005).
10. L. Kondic and J. A. Diez, Phys. Rev. E **79**, 026302 (2009).
11. C. Favazza, J. Trice, H. Krishna, and R. Kalyanaraman, Appl. Phys. Lett. **88**, 153118 (2006).
12. K. L. Kelly, E. Coronado, L. L. Zhao, and G. C. Schatz, J. Phys. Chem. B **107**, 668 (2003).
13. Y. J. Liu, Z. Y. Zhang, Q. Zhao, and Y. P. Zhao, Appl. Phys. Lett. **93**, 173106 (2008).
14. P. A. Temple and C. E. Hathaway, Phys. Rev. B **7**, 3685 (1973).
15. R. P. Van Duyne, J. C. Hulteen, and D. A. Treichel, J. Chem. Phys. **99**, 2101 (1993).